

**All-optical manipulation of charge density waves in kagome metal CsV<sub>3</sub>Sb<sub>5</sub>**Junhong Yu,<sup>1</sup> Yadong Han,<sup>1,2</sup> Qiangwei Yin,<sup>3</sup> Zhengwei Nie,<sup>4</sup> Longyu Wang,<sup>1,2</sup> Chunsheng Gong,<sup>3</sup> Zhijun Tu,<sup>3</sup> Fang Xu,<sup>2</sup> Yonggang Liu,<sup>2</sup> Hang Zhang,<sup>1,2</sup> Oleg V. Misochko,<sup>5</sup> Sheng Meng,<sup>4,\*</sup> Hechang Lei,<sup>3,†</sup> and Jianbo Hu<sup>1,2,‡</sup><sup>1</sup>Laboratory for Shock Wave and Detonation Physics, Institute of Fluid Physics, China Academy of Engineering Physics, Mianyang 621900, China<sup>2</sup>State Key Laboratory for Environment-Friendly Energy Materials, Southwest University of Science and Technology, Mianyang 621010, China<sup>3</sup>Department of Physics and Beijing Key Laboratory of Opto-electronic Functional Materials & Micro-nano Devices, Renmin University of China, Beijing 100872, China<sup>4</sup>Beijing National Laboratory for Condensed Matter Physics, Institute of Physics, Chinese Academy of Sciences, Beijing 100190, China<sup>5</sup>Institute of Solid State Physics, Russian Academy of Sciences, 142432 Chernogolovka, Moscow Region, Russia

(Received 6 September 2022; accepted 24 April 2023; published 5 May 2023)

A major challenge in condensed matter physics is to manipulate collective quantum phases by all-optical methods, which can open enormous new possibilities for materials and device engineering. Here we report an anomalous optical modulation of charge density waves (CDWs) in recently discovered kagome metal CsV<sub>3</sub>Sb<sub>5</sub> using femtosecond-resolved coherent phonon spectroscopy. This optically suppressed CDW phase surprisingly persists for nanoseconds, exhibits a monotonically lowering of transition temperature with increasing fluence, and does not require a critical absorbed photon density, which is intriguingly distinct from those found in the “optically suppressed potential energy” scenario. Pump-pump-probe experiments conclusively rule out the laser-induced thermal effect and time-dependent density functional theory simulations confirm that this nonthermal modulation stems from an optical tuning of the energy resonance between the band fermiology and the Van Hove singularity in kagome lattices. These findings open exciting prospects for all-optical engineering of the Van Hove scenario to tune correlated quantum phases in topology networks.

DOI: [10.1103/PhysRevB.107.174303](https://doi.org/10.1103/PhysRevB.107.174303)**I. INTRODUCTION**

It is well known that when the Fermi energy ( $E_F$ ) approaches the Van Hove singularity (VHs) in electronic band structure (i.e., the so-called Van Hove scenario), electronic interactions are drastically amplified by the divergent density of states (DOS), leading to new phases of matter with exotic properties [1–3]. This physical concept inspires enormous experimental demonstrations of correlated electron phenomena (e.g., the discovery of unconventional insulating states and superconductivity in twisted bilayer graphene [4,5]) and has been further utilized as an intriguing avenue to statically engineering collective quantum phenomena in various material systems (e.g., tuning the energy resonance between VHs and the band fermiology via chemical doping, electronic gating, or superlattice construction [3,6–9]). However, an important path forward is to dynamically tune the Van Hove scenario using an optical pulse, which may achieve novel correlated electron phases that persist, far from equilibrium, and are inaccessible by conventional static tuning approaches [10,11].

In this regard, quantum materials with a kagome lattice, which naturally support VHs and flat bands with diverg-

ing density of states (DOS), have been intensively explored in a series of 3d-transition metal compounds, including TbMn<sub>6</sub>Sn<sub>6</sub> [12,13] (Fe, Co)Sn [14,15] and Co<sub>3</sub>Sn<sub>2</sub>S<sub>2</sub> [16,17]. Unfortunately, the absence of the Van Hove scenario in all Mn-, Fe-, and Co-based kagome metals (e.g., their VHs located too far away from the Fermi energy) makes the manipulation of collective electronic correlations elusive. Recent discoveries of AV<sub>3</sub>Sb<sub>5</sub> (A = K, Rb, Cs) as a family of non-magnetic kagome metals open fascinating possibilities for engineering the Van Hove scenario considering that these compounds not only exhibit rich correlated ground states including bulk superconductivity and inverse Star of David charge density waves (CDWs) [18–24] but also support a close energy resonance between the Van Hove singularities at  $M$  points and the  $d_{xz}/d_{yz}$  band fermiology of V atoms [21,24–26].

Here, we utilize ultrafast coherent phonon spectroscopy to investigate the possibility of optically manipulating the charge density order in kagome metal CsV<sub>3</sub>Sb<sub>5</sub>. Comprehensive temperature and excitation density-dependent coherent phonon behaviors reveal an unexpected manipulation of the CDW state with photoexcitation, which persists over nanoseconds, is absent of threshold, and exhibits a monotonic lowering of transition temperature ( $T_{CDW}$ ) with increasing excitation fluence. These results are dramatically different from those found in optical suppression of CDW based on the “photoexcitation modified potential energy” mechanism [27,28]. Furthermore, pump-pump-probe experiments confirm that the 12.5 ns time interval for our laser repetition rate is long enough to dissipate the cumulative heating between two

\* Author to whom correspondence should be addressed: smeng@iphy.ac.cn

† Author to whom correspondence should be addressed: hlei@ruc.edu.cn

‡ Author to whom correspondence should be addressed: jianbo.hu@caep.cn

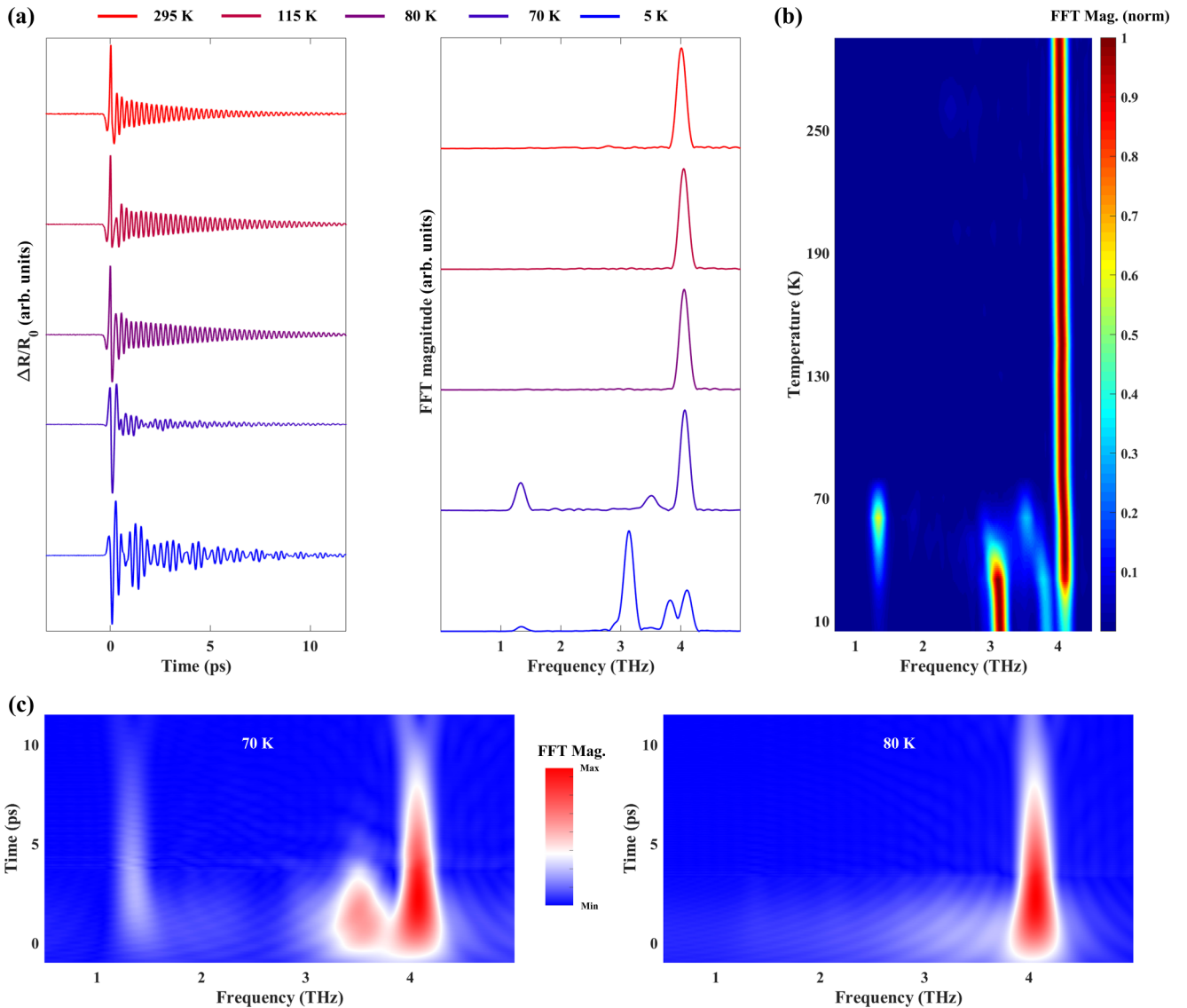


FIG. 1. Temperature-dependent coherent phonon spectra of  $\text{CsV}_3\text{Sb}_5$  with the pump fluence ( $F$ ) of  $\sim 3.2 \mu\text{J}/\text{cm}^2$ . (a) Transient photoinduced coherent oscillations after subtracting the incoherent electronic response (the left panel) and corresponding FFTs (the right panel). The curves are offset vertically for clarity. (b) Normalized two-dimensional color map of the Fourier transform as a function of temperature and frequency. Two charge density orders with distinct transition temperatures can be resolved. (c) Sliding window FT (SWFT) for  $T = 80 \text{ K}$  (right panel) and  $T = 70 \text{ K}$  (left panel). At  $80 \text{ K}$  (below the equilibrium CDW transition temperature), the absence of the recovery process in the measured time window is observed.

adjacent pump pulses, which eliminates the contribution of cumulative laser heating effects and validates the nonthermal nature of our observations. Combining experimental results with theoretical modelings, we argue that such an anomalous modulation of CDW states in  $\text{CsV}_3\text{Sb}_5$  originates from the optical tuning of the Van Hove scenario.

## II. RESULTS

Single crystals of  $\text{CsV}_3\text{Sb}_5$  with shining surfaces are grown by a self-flux method (see Supplemental Material, Note 1 [29]; also see [18,19,30–40]) similar to previous reports [18,41]. The atomic structure of  $\text{CsV}_3\text{Sb}_5$  comprises stacking of Cs-Sb<sub>2</sub>-VSb<sub>1</sub>-Sb<sub>2</sub>-Cs layers with hexagonal symmetry (space group  $P6/mmm$ ; see Supplemental Mate-

rial, Fig. S1 [29]). Various equilibrium measurements have confirmed that the low energy physics of  $\text{CsV}_3\text{Sb}_5$  is dominated by a three-dimensional CDW phase transition at  $T_{\text{CDW}} \approx 94 \text{ K}$  [18–22,25,26]. In our work, the nonequilibrium properties of this material are revealed by femtosecond-resolved coherent phonon spectroscopy [42–44]. A commercial Ti:sapphire amplifier producing 20 fs laser pulses at 800 nm with an 80 MHz repetition is used as a source of both pump and probe pulse trains. The pump laser beam is polarized along the perpendicular direction (the  $c$  axis) while the polarization of the probe beam is set orthogonal to the pump beam to eliminate coherent artifacts. More experimental details are presented in the Supplemental Material, Note 2 [29]). The coherent atomic oscillations of  $\text{CsV}_3\text{Sb}_5$  upon photoexcitation at different temperatures with a fluence of

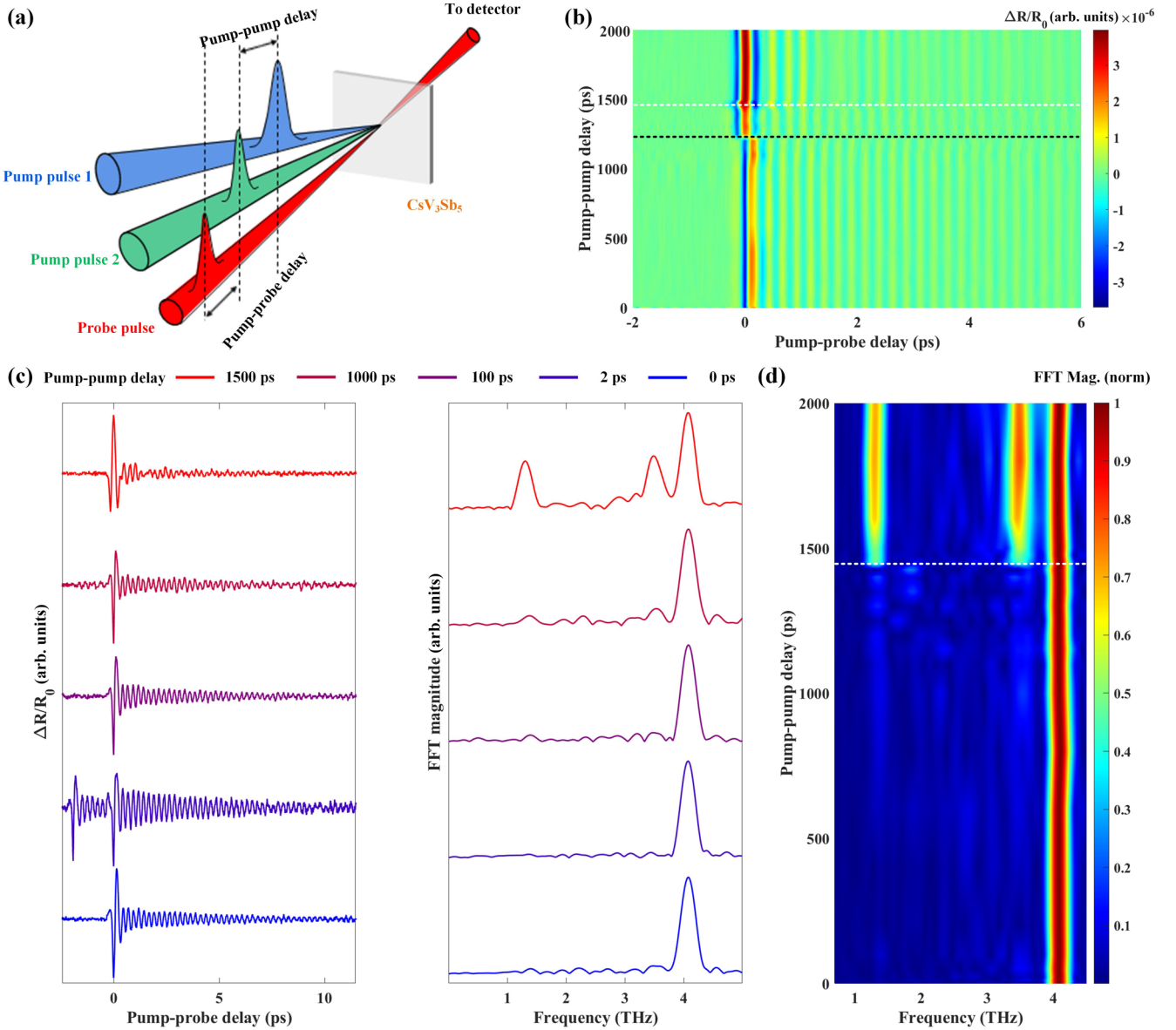


FIG. 2. Pump-pump-probe coherent phonon spectra of CsV<sub>3</sub>Sb<sub>5</sub> at 80 K. (a) Schematic of the three-pulse experiment. The fluence of each pump pulse is  $\sim 1.6 \mu\text{J}/\text{cm}^2$ . More details of the pump-pump-probe experiment are provided in Supplemental Material, Note 2 [29]. (b) Normalized two-dimensional color map of transient photoinduced coherent oscillations as a function of the pump-pump delay and the pump-probe delay. The white dashed line marks the pump-pump delay time when the peak value of  $\Delta R/R_0$  flips the sign. The black dashed line marks the pump-pump delay time when the multiple-mode oscillation occurs. (c) Transient photoinduced coherent oscillations (left panel) and corresponding FFTs (right panel) at five representative pump-pump delay times. (d) Normalized two-dimensional color map of the Fourier transform as a function of the pump-pump delay and frequency. The white dashed line marks the pump-pump delay time when the multiple-mode oscillation occurs.

$\sim 3.2 \mu\text{J}/\text{cm}^2$  are presented in the left panel of Fig. 1(a), where the incoherent signal has been removed by subtracting the exponential fitting of the electronic decay process [45–47]. The corresponding fast Fourier transforms (FFTs) are shown in the right panel of Fig. 1(a). It can be seen that at temperatures beyond 80 K, only one phonon mode with a frequency of  $\sim 4.0$  THz is detected, which agrees with the recent Raman study [24,48] and density functional calculations [49] for the  $A_{1g}$  phonon mode. When the temperature goes down to 70 K, additional oscillation modes show up with frequencies of  $\sim 1.3$ ,  $\sim 2.9$ , and  $\sim 3.5$  THz. Based on symmetry analy-

sis [49,50], the phonon mode at  $\sim 2.9$  THz is either  $M_4^-$  or  $L_3^+$  (the notation of Miller and Love); while phonon modes at  $\sim 1.3$  and  $\sim 3.5$  THz are either  $M_1^+$  or  $L_2^-$ , which can be assigned as the  $E_{1g}$  and  $E_{2g}$  mode, respectively.

More information can be recognized from the temperature-dependent color map of FFTs in Fig. 1(b). Here several effects are visible: (1) Three additional coherent phonon modes appear abruptly just below a critical temperature at  $\sim 74$  K, implying that they are highly related to the CDW structural modulation [50]. And very surprisingly,  $T_{\text{CDW}}$  based on the appearance of these three additional modes is significantly lower

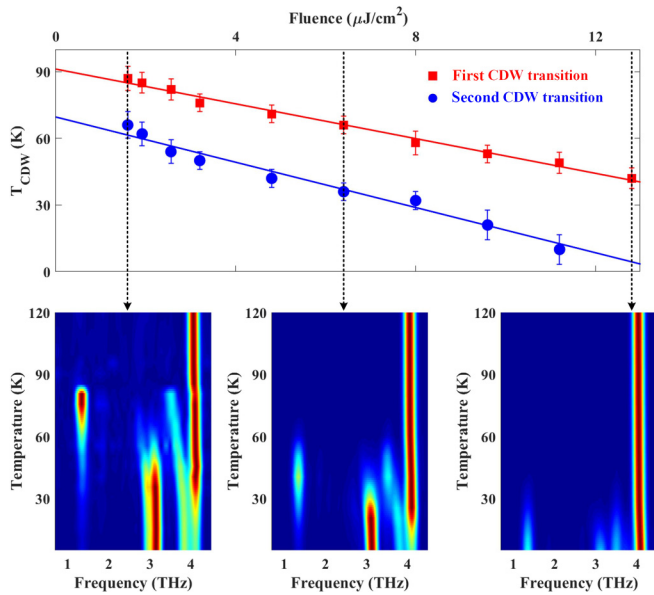


FIG. 3. Fluence-dependent CDW states. Upper panel: Fluence-dependent transition temperature of the first and the second CDW state. The dashed line is a guide to the eye. Bottom panel: Three representative 2D coherent phonon maps for  $F = 1.6 \mu\text{J}/\text{cm}^2$  (left panel),  $F = 6.4 \mu\text{J}/\text{cm}^2$  (middle panel), and  $F = 12.8 \mu\text{J}/\text{cm}^2$  (right panel), which exhibit a distinct transition temperature.

than the thermal equilibrium value ( $\sim 94$  K), implying that photoexcitation can modulate the CDW phase in  $\text{CsV}_3\text{Sb}_5$ . (2) Phonon modes at  $\sim 2.9$  and  $\sim 3.5$  THz exhibit a weak frequency softening upon approaching  $\sim 74$  K, and proceed in a fashion very similar to the Bardeen-Cooper-Schrieffer (BCS) gap function [51,52] (see the temperature-dependent phonon mode analysis in the Supplemental Material, Fig. S2 [29]), indicating that these two modes are probably the amplitude mode of charge ordering. (3) There exists a second critical transition temperature ( $\sim 50$  K), at which the frequency of the  $\sim 3.5$  THz mode undergoes a sudden discrete shift and the amplitude of the  $\sim 1.3$  THz mode becomes heavily divergent (see Fig. 1(b) and Supplemental Material, Fig. S2 [29]). This behavior is suggested to be related to the uniaxial charge ordering observed in scanning tunneling microscopy experiments [22,41] which demonstrate the symmetry change in  $\text{CsV}_3\text{Sb}_5$  from  $C_6$  to  $C_2$  at  $T \approx 60$  K.

Another intriguing part of the photoexcitation modulated CDW phase in  $\text{CsV}_3\text{Sb}_5$  is resolved in the time-dependent phonon mode spectra obtained by sliding window FT (see Fig. 1(c) and the Supplemental Material, Note 3 [29]), which yields instantaneous frequencies and amplitudes of the coherent oscillations [53–55]. As can be seen in the chronogram at 80 K, which is already below the thermal-equilibrium CDW transition temperature ( $\sim 94$  K), only the  $A_{1g}$  optical phonon mode at  $\sim 4.0$  THz can be observed throughout the entire time window (for reference, the chronogram at 70 K is also provided in Fig. 1(c) where additional coherent oscillations can be observed). It suggests a long-lived photoinduced change in the charge ordering and is distinct from previous ultrafast photomodulation works which typically recover in a subpicosecond timescale [27]. Please note that laser pulse

excitation does not yield a permanent modulation of charge ordering in  $\text{CsV}_3\text{Sb}_5$  and the coherent phonon spectra will recover to the initial state whenever the pump fluence is tuned back to small values (see Supplemental Material, Fig. S3 [29]), ruling out the possibility of photoinduced hidden quantum states as observed in  $1T\text{-TaS}_2$  [10,56].

Now, a legitimate question would be “are these anomalous features originating from the trivial laser-induced heating effects?” since the simplest explanation for a lower  $T_{\text{CDW}}$  and the long-lived modulation is that pronounced cumulative heating makes the temperature of the probed spot higher than that of the cryostat cold finger. As shown in Fig. 2(a), we have conducted a three-pulse experiment to rule out this possibility [43,57]. Specifically, the  $\text{CsV}_3\text{Sb}_5$  sample at 80 K is excited by two identical pump pulses (fluence of each:  $1.6 \mu\text{J}/\text{cm}^2$ ) with different incident angles to avoid the optical interference effect and by varying the pump-pump delay ( $t_{\text{pp}}$ ), we can therefore investigate the role of incomplete heat dissipation between pump pulses on the CDW state (more experimental details are provided in the Supplemental Material, Note 4 [29]). From the measured reflectivity time trace (see Fig. 2(b), the left panel of Fig. 2(c), and Supplemental Material, Fig. S4 [29]), the single-mode oscillation is observed with a small  $t_{\text{pp}}$  which is similar to one-pulse excitation with a fluence of  $3.2 \mu\text{J}/\text{cm}^2$  at 80 K, while with  $t_{\text{pp}}$  larger than  $\sim 1150$  ps, the peak value of  $\Delta R/R_0$  flips the sign from negative to positive [30,49] and the oscillation finally changes to a multiple-mode behavior at  $\sim 1425$  ps. We can also obtain similar information by performing frequency domain analysis with different pump-pump delays (see the right panel of Figs. 2(c) and 2(d), and the Supplemental Material, Fig. S5 [29]), in which the FFT spectrum transits from the single mode into the multiple mode at  $\sim 1425$  ps, implying that the optically suppressed CDW state has recovered.

From the thermal effect point of view, the above observations can be understood as follows. For early pump-pump delay ( $< \sim 1.4$  ns), only the single-mode oscillation is observed, suggesting that the combined steady-state heating effect of two pump pulses when they are close in the time domain effectively raises the sample temperature above the thermal equilibrium  $T_{\text{CDW}}$  ( $\sim 94$  K). However, if the second pump pulse arrives after  $\sim 1.4$  ns, the remaining heat from the first pump pulse has sufficiently dissipated so that the cumulative steady-state heating effect is suppressed and multimode oscillations are observed. If this explanation is valid (i.e., the heat dissipation time for an individual laser pulse is about  $\sim 1.4$  ns in  $\text{CsV}_3\text{Sb}_5$  at 80 K), the 12.5 ns time interval for the 80 MHz repetition rate in Fig. 1 should be long enough to dissipate the cumulative heating between two adjacent pump pulses, which is contradicted with the steady-state thermal scenario. It is worth mentioning that we have calculated the sample temperature rise induced by the pump pulse [30,58] (see details in the Supplemental Material, Note 5 [29]) and a small estimated value ( $< 2$  K) also indicates an insignificant role of the cumulative laser heating. Hence, we can confirm that the photoinduced modulation of CDW states in  $\text{CsV}_3\text{Sb}_5$  is nonthermal in origin and this modulation can persist for nanoseconds.

To gain additional insights into the optical modulation of charge ordering in  $\text{CsV}_3\text{Sb}_5$ , the fluence-dependent

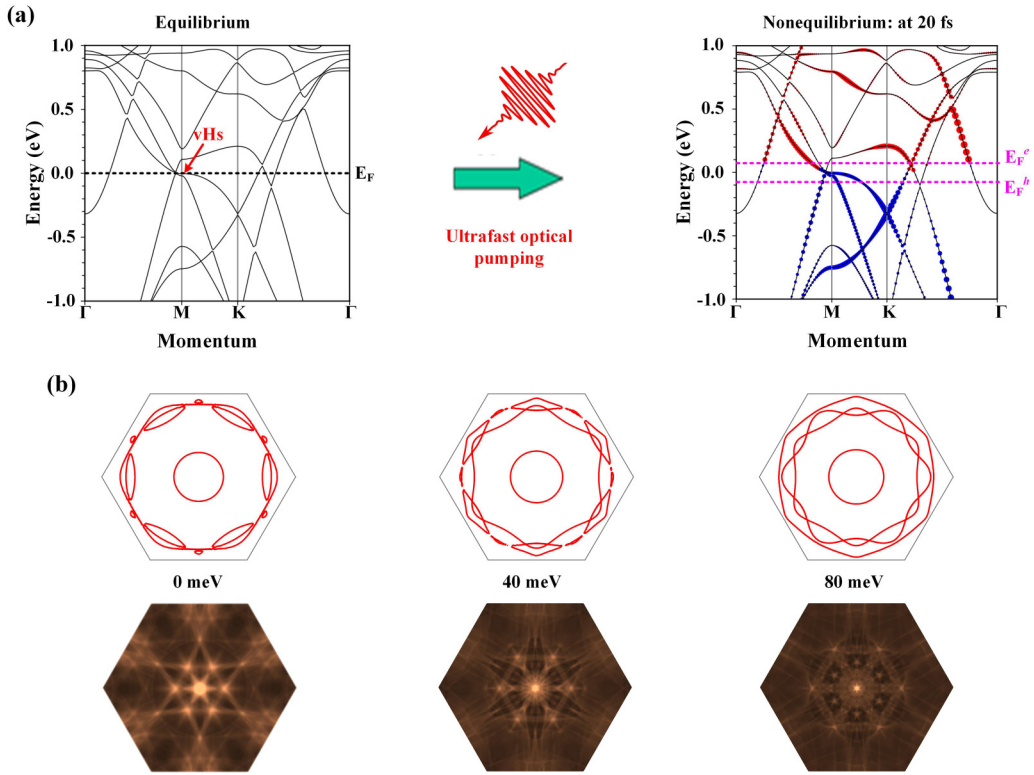


FIG. 4. A possible mechanism to explain anomalous optical modulation. (a) A schematic to show optical tuning of the Van Hove scenario in  $\text{CsV}_3\text{Sb}_5$ . Nonequilibrium Fermi energy shifting after optical pumping change suppresses the electronic correlations in the kagome lattice.  $E_F^e$  and  $E_F^h$  denote the quasi-Fermi energy of electrons and holes under nonequilibrium condition, respectively. (b) The calculated Fermi surface change and the imaginary part of electric susceptibility (a measure of the charge ordering strength) with different Fermi level shifting.

coherent phonon spectra have been investigated. In Fig. 3, temperature-dependent color maps of FFTs with three representative fluences are presented, from which we can see that the appearance temperature of additional phonon modes and the occurrence temperature of anomalies in  $\sim 1.3/\sim 3.5$  THz modes vary with different fluences. It implies that there is a noticeable decrease in the transition temperature for both CDW states with increasing fluences (e.g., the second CDW transition becomes even unresolvable for  $F = 12.8 \mu\text{J}/\text{cm}^2$ ). This argument can be seen more obviously in the fluence-dependent transition temperatures of the first ( $T_{\text{CDW}1}$ ) and second ( $T_{\text{CDW}2}$ ) CDW states. As the fluence increases, the transition temperatures of both CDW phases go through a continuous and monotonic decrease with a similar slope ( $\sim 3.5 \text{ K cm}^2/\mu\text{J}$ ). This similarity indicates that the modulation mechanism should be generally suitable for electronic correlations in  $\text{CsV}_3\text{Sb}_5$ , which does not discriminate against different structure symmetry (i.e.,  $C_6$  and  $C_2$ ) [22] or diverse energy minima in the potential energy surface [59]. At this stage, we speculate that the optically modulated charge ordering should be closely related to the density of excited electrons. Moreover, we find that surprisingly no threshold fluence is required for the photomodulated  $T_{\text{CDW}}$  down to the lowest fluence level for our setup to obtain reliable data ( $\sim 1.6 \mu\text{J}/\text{cm}^2$ ). If linearly extrapolating the photomodulated  $T_{\text{CDW}}$  to  $F = 0 \mu\text{J}/\text{cm}^2$ , a calculated  $T_{\text{CDW}}$  of the first CDW state ( $90.8 \pm 4.7 \text{ K}$ ) without excitation is in good agreement with the transition temperature ( $\sim 94 \text{ K}$ ) in thermal equilibrium measurements. The absence of an excitation threshold

suggests a unique photoinduced effect different from previous nonequilibrium modulation works (e.g., in  $\text{VO}_2$  [60],  $\text{TaS}_2$  [10],  $\text{MoTe}_2$  [61],  $\text{WTe}_2$  [62],  $\text{K}_0.3\text{MoO}_3$  [31], and  $\text{Ta}_2\text{NiSe}_5$  [56,57]), in which a certain intensity of the pump field is required to overcome the potential energy barrier and prevent the lattice from recovering to its original state.

### III. DISCUSSION

We have experimentally demonstrated that ultrafast photoexcitation can nonthermally modulate CDW phases in  $\text{CsV}_3\text{Sb}_5$  with several peculiar features, namely, the long-lived optical suppression, a monotonically lowering of  $T_{\text{CDW}}$  with increasing fluence, and the absence of excitation threshold. With the recent development of time-resolved probes, optical suppression of CDW phases has been observed with intense laser pulse excitations [27,28,31–33], which can be well explained by the photoexcitation modified potential energy mechanism depicted in the Supplemental Material, Fig. S6 [29]. However, the behavior of charge ordering under the above-mentioned scenario is inconsistent with our experimental observations. First of all, after the local equilibrium is established by electron-electron scatterings, the electronic subsystem will quickly cool down via phonon-assisted electron relaxation, accompanied by the rapid recovery of photomodulated potential energy [27]. Thereby an ultrafast recovery process is commonly observed, which typically takes place on the subpicosecond to picosecond timescale [27,31–33]. Secondly, the excitation density required to optically

suppress the charge ordering should be able to overcome the energy barrier between the normal metallic state and the CDW state [56,57]; therefore, an excitation threshold was required in previous works [27,28,31–33]. Lastly but importantly, the “photoinduced potential energy change” scenario also fails to explain the similar and simultaneous modulation of two CDW phases (i.e., the  $2a_0$  tridirectional and  $4a_0$  unidirectional charge ordering) [22] with distinct potential energy surface and different equilibrium atomic positions in  $\text{CsV}_3\text{Sb}_5$ .

To understand the origin of this anomalous optical modulation, we have performed nonadiabatic molecular dynamics (MD) simulations based on time-dependent density functional theory (simulation details are given in the Supplemental Material, Note 6 [29,63–70]). As illustrated in Fig. 4(a), a Van Hove singularity that stems from  $d_{xz}/d_{yz}$  orbitals of V atoms is most vital to the charge ordering in  $\text{CsV}_3\text{Sb}_5$ , since the vector of the  $2 \times 2$  superlattice charge modulation connects the Van Hove singularities at  $M$  points and matches with the fermiology of the  $d_{xz}/d_{yz}$  band [25]. Under ultrafast photoexcitation, excited carriers are likely to occupy orbitals near saddle points (see the calculated carrier occupation in Fig. 4(a) and Supplemental Material, Fig. S7 [29]), which will correspondingly disturb the equilibrium band fermiology and suppress the electronic correlations. Figure 4(b) has presented the Fermi surface of  $k_z = 0$  and the corresponding imaginary part of the electric susceptibility (i.e., a measure for electronic correlations) [34] with the Fermi energy shifting ( $E_F^{\text{shift}}$ ) of 0, 40, and 80 meV, respectively. It can be seen that under the ground state (i.e.,  $E_F^{\text{shift}} = 0$  meV), the charge ordering strength has a maximum around saddle points  $M$ , while with increasing  $E_F^{\text{shift}}$ , the charge ordering strength is weakened, therefore shifting the transition temperature downward. Meanwhile, since the nonequilibrium Fermi level shifting is proportional to the excited electron density [35], the absence of threshold and a monotonical decrease of  $T_{\text{CDW}}$  with the increasing fluence

can be well explained. Moreover, as demonstrated in our works, the energy shifting of the Fermi level can significantly modulate the Van Hove scenario and correspondingly change the status of charge ordering. Therefore, the recovery process of the quasi-Fermi level determines the lasting timescale of this photoinduced modulation. Here we argue that the slow recovery process of the optically modulated CDW phases in  $\text{CsV}_3\text{Sb}_5$  may be due to the excited carrier localization scenario: A singularity (nonsmooth point) in the density of states (DOS) will accumulate carriers and slow down the interband scattering process at the edges of the electron bands due to the density of states effects and Pauli blocking. As a result, a slowing down of the quasi-Fermi level due to the excited carrier localization scenario at saddle point  $M$  is expected.

In summary, the experiments described here demonstrate that in kagome metal  $\text{CsV}_3\text{Sb}_5$  one can effectively tune the CDW phase by a weak laser pulse with distinct features including the absence of excitation threshold, a monotonic decrease of  $T_{\text{CDW}}$  with increasing fluences, and an ultra-slow recovery process, which are attributed to photoexcitation modulated energy resonance between the band fermiology and the Van Hove singularity in kagome lattices. Our observations highlight the role of band topology in emergent electronic phenomena and may provide enlightenment for nonequilibrium manipulation of exotic quantum phenomena.

#### ACKNOWLEDGMENTS

This work was supported by the Science Challenge Project (Grant No. TZ2018001), the National Natural Science Foundation of China (Grants No. 12072331, No. 11822412, and No. 11774423), the National Key R&D Program of China (Grant No. 2018YFE0202600), and Beijing Natural Science Foundation (Grant No. Z200005).

- [1] W. Kohn and J. Luttinger, New Mechanism for Superconductivity, *Phys. Rev. Lett.* **15**, 524 (1965).
- [2] T. Rice and G. Scott, New Mechanism for a Charge-Density-Wave Instability, *Phys. Rev. Lett.* **35**, 120 (1975).
- [3] G. Li, A. Luican, J. Lopes dos Santos, A. Castro Neto, A. Reina, J. Kong, and E. Andrei, Observation of Van Hove singularities in twisted graphene layers, *Nat. Phys.* **6**, 109 (2010).
- [4] Y. Cao, V. Fatemi, S. Fang, K. Watanabe, T. Taniguchi, E. Kaxiras, and P. Jarillo-Herrero, Unconventional superconductivity in magic-angle graphene superlattices, *Nature (London)* **556**, 43 (2018).
- [5] Y. Cao, V. Fatemi, A. Demir, S. Fang, S. L. Tomarken, J. Y. Luo, J. D. Sanchez-Yamagishi, K. Watanabe, T. Taniguchi, and E. Kaxiras, Correlated insulator behaviour at half-filling in magic-angle graphene superlattices, *Nature (London)* **556**, 80 (2018).
- [6] A. J. Jones, R. Muzzio, P. Majchrzak, S. Pakdel, D. Curcio, K. Volckaert, D. Biswas, J. Gobbo, S. Singh, and J. T. Robinson, Observation of electrically tunable Van Hove singularities in twisted bilayer graphene from NanoARPES, *Adv. Mater.* **32**, 2001656 (2020).
- [7] D. Yudin, D. Hirschmeier, H. Hafermann, O. Eriksson, A. I. Lichtenstein, and M. I. Katsnelson, Fermi Condensation near Van Hove Singularities within the Hubbard Model on the Triangular Lattice, *Phys. Rev. Lett.* **112**, 070403 (2014).
- [8] S. Xu, M. M. Al Ezzi, N. Balakrishnan, A. Garcia-Ruiz, B. Tsim, C. Mullan, J. Barrier, N. Xin, B. A. Piot, and T. Taniguchi, Tunable Van Hove singularities and correlated states in twisted monolayer–bilayer graphene, *Nat. Phys.* **17**, 619 (2021).
- [9] N. F. Yuan, H. Isobe, and L. Fu, Magic of high-order Van Hove singularity, *Nat. Commun.* **10**, 5769 (2019).
- [10] L. Stojchevska, I. Vaskivskiy, T. Mertelj, P. Kusar, D. Svetin, S. Brazovskii, and D. Mihailovic, Ultrafast switching to a stable hidden quantum state in an electronic crystal, *Science* **344**, 177 (2014).
- [11] J. Zhang, X. Tan, M. Liu, S. W. Teitelbaum, K. W. Post, F. Jin, K. A. Nelson, D. N. Basov, W. Wu, and R. D. Averitt, Cooperative photoinduced metastable phase control in strained manganite films, *Nat. Mater.* **15**, 956 (2016).
- [12] X. Xu, J.-X. Yin, W. Ma, H.-J. Tien, X.-B. Qiang, P. S. Reddy, H. Zhou, J. Shen, H.-Z. Lu, and T.-R. Chang, Topological

- charge-entropy scaling in kagome Chern magnet  $\text{TbMn}_6\text{Sn}_6$ , *Nat. Commun.* **13**, 1197 (2022).
- [13] J.-X. Yin, W. Ma, T. A. Cochran, X. Xu, S. S. Zhang, H.-J. Tien, N. Shumiya, G. Cheng, K. Jiang, and B. Lian, Quantum-limit Chern topological magnetism in  $\text{TbMn}_6\text{Sn}_6$ , *Nature (London)* **583**, 533 (2020).
- [14] M. Kang, L. Ye, S. Fang, J.-S. You, A. Levitan, M. Han, J. I. Facio, C. Jozwiak, A. Bostwick, and E. Rotenberg, Dirac fermions and flat bands in the ideal kagome metal  $\text{FeSn}$ , *Nat. Mater.* **19**, 163 (2020).
- [15] M. Kang, S. Fang, L. Ye, H. C. Po, J. Denlinger, C. Jozwiak, A. Bostwick, E. Rotenberg, E. Kaxiras, and J. G. Checkelsky, Topological flat bands in frustrated kagome lattice  $\text{CoSn}$ , *Nat. Commun.* **11**, 4004 (2020).
- [16] Q. Wang, Y. Xu, R. Lou, Z. Liu, M. Li, Y. Huang, D. Shen, H. Weng, S. Wang, and H. Lei, Large intrinsic anomalous Hall effect in half-metallic ferromagnet  $\text{Co}_3\text{Sn}_2\text{S}_2$  with magnetic Weyl fermions, *Nat. Commun.* **9**, 3681 (2018).
- [17] Y. Okamura, S. Minami, Y. Kato, Y. Fujishiro, Y. Kaneko, J. Ikeda, J. Muramoto, R. Kaneko, K. Ueda, and V. Kocsis, Giant magneto-optical responses in magnetic Weyl semimetal  $\text{Co}_3\text{Sn}_2\text{S}_2$ , *Nat. Commun.* **11**, 4619 (2020).
- [18] B. R. Ortiz, L. C. Gomes, J. R. Morey, M. Winiarski, M. Bordelon, J. S. Mangum, I. W. Oswald, J. A. Rodriguez-Rivera, J. R. Neilson, and S. D. Wilson, New kagome prototype materials: Discovery of  $\text{KV}_3\text{Sb}_5$ ,  $\text{RbV}_3\text{Sb}_5$ , and  $\text{CsV}_3\text{Sb}_5$ , *Phys. Rev. Mater.* **3**, 094407 (2019).
- [19] B. R. Ortiz, S. M. Teicher, Y. Hu, J. L. Zuo, P. M. Sarte, E. C. Schueller, A. M. Abeykoon, M. J. Krogstad, S. Rosenkranz, and R. Osborn,  $\text{CsV}_3\text{Sb}_5$ : A  $Z_2$  Topological Kagome Metal with a Superconducting Ground State, *Phys. Rev. Lett.* **125**, 247002 (2020).
- [20] H. Tan, Y. Liu, Z. Wang, and B. Yan, Charge Density Waves and Electronic Properties of Superconducting Kagome Metals, *Phys. Rev. Lett.* **127**, 046401 (2021).
- [21] Y. Hu, X. Wu, B. R. Ortiz, S. Ju, X. Han, J. Ma, N. C. Plumb, M. Radovic, R. Thomale, and S. D. Wilson, Rich nature of Van Hove singularities in kagome superconductor  $\text{CsV}_3\text{Sb}_5$ , *Nat. Commun.* **13**, 2220 (2022).
- [22] H. Zhao, H. Li, B. R. Ortiz, S. M. Teicher, T. Park, M. Ye, Z. Wang, L. Balents, S. D. Wilson, and I. Zeljkovic, Cascade of correlated electron states in the kagome superconductor  $\text{CsV}_3\text{Sb}_5$ , *Nature (London)* **599**, 216 (2021).
- [23] H. Luo, Q. Gao, H. Liu, Y. Gu, D. Wu, C. Yi, J. Jia, S. Wu, X. Luo, and Y. Xu, Electronic nature of charge density wave and electron-phonon coupling in kagome superconductor  $\text{KV}_3\text{Sb}_5$ , *Nat. Commun.* **13**, 273 (2022).
- [24] G. Liu, X. Ma, K. He, Q. Li, H. Tan, Y. Liu, J. Xu, W. Tang, K. Watanabe, and T. Taniguchi, Observation of anomalous amplitude modes in the kagome metal  $\text{CsV}_3\text{Sb}_5$ , *Nat. Commun.* **13**, 3461 (2022).
- [25] M. Kang, S. Fang, J. K. Kim, B. R. Ortiz, S. H. Ryu, J. Kim, J. Yoo, G. Sangiovanni, D. Di Sante, and B. G. Park, Twofold Van Hove singularity and origin of charge order in topological kagome superconductor  $\text{CsV}_3\text{Sb}_5$ , *Nat. Phys.* **18**, 301 (2022).
- [26] M. M. Denner, R. Thomale, and T. Neupert, Analysis of Charge Order in the Kagome Metal  $\text{AV}_3\text{Sb}_5$  ( $A = \text{K}, \text{Rb}, \text{Cs}$ ), *Phys. Rev. Lett.* **127**, 217601 (2021).
- [27] M. Eichberger, H. Schäfer, M. Krumova, M. Beyer, J. Demsar, H. Berger, G. Moriena, G. Sciaini, and R. D. Miller, Snapshots of cooperative atomic motions in the optical suppression of charge density waves, *Nature (London)* **468**, 799 (2010).
- [28] J. Maklar, Y. W. Windsor, C. W. Nicholson, M. Puppini, P. Walmsley, V. Esposito, M. Porer, J. Rittmann, D. Leuenberger, and M. Kubli, Nonequilibrium charge-density-wave order beyond the thermal limit, *Nat. Commun.* **12**, 2499 (2021).
- [29] See Supplemental Material at <http://link.aps.org/supplemental/10.1103/PhysRevB.107.174303> for additional information on crystal structure, temperature-phonon mode analysis, pump-pump-probe coherent phonon spectroscopy, SWFT, estimation of thermal effect, and numerical calculations, which includes Refs. [18,19,30–40].
- [30] Z. Wang, Q. Wu, Q. Yin, C. Gong, Z. Tu, T. Lin, Q. Liu, L. Shi, S. Zhang, and D. Wu, Unconventional charge density wave and photoinduced lattice symmetry change in the kagome metal  $\text{CsV}_3\text{Sb}_5$  probed by time-resolved spectroscopy, *Phys. Rev. B* **104**, 165110 (2021).
- [31] A. Tomeljak, H. Schaefer, D. Städter, M. Beyer, K. Biljakovic, and J. Demsar, Dynamics of Photoinduced Charge-Density-Wave to Metal Phase Transition in  $\text{K}_{0.3}\text{MoO}_3$ , *Phys. Rev. Lett.* **102**, 066404 (2009).
- [32] E. Möhr-Vorobeva, S. L. Johnson, P. Beaud, U. Staub, R. De Souza, C. Milne, G. Ingold, J. Demsar, H. Schäfer, and A. Titov, Nonthermal Melting of a Charge Density Wave in  $\text{TiSe}_2$ , *Phys. Rev. Lett.* **107**, 036403 (2011).
- [33] S. Hellmann, T. Rohwer, M. Kalläne, K. Hanff, C. Sohrt, A. Stange, A. Carr, M. Murnane, H. Kapteyn, and L. Kipp, Time-domain classification of charge-density-wave insulators, *Nat. Commun.* **3**, 1069 (2012).
- [34] M. Johannes and I. Mazin, Fermi surface nesting and the origin of charge density waves in metals, *Phys. Rev. B* **77**, 165135 (2008).
- [35] Y. Wang, D. Hsieh, E. Sie, H. Steinberg, D. Gardner, Y. Lee, P. Jarillo-Herrero, and N. Gedik, Measurement of Intrinsic Dirac Fermion Cooling on the Surface of the Topological Insulator  $\text{Bi}_2\text{Se}_3$  Using Time-Resolved and Angle-Resolved Photoemission Spectroscopy, *Phys. Rev. Lett.* **109**, 127401 (2012).
- [36] X. Zhou, Y. Li, X. Fan, J. Hao, Y. Dai, Z. Wang, Y. Yao, and H.-H. Wen, Origin of charge density wave in the kagome metal  $\text{CsV}_3\text{Sb}_5$  as revealed by optical spectroscopy, *Phys. Rev. B* **104**, L041101 (2021).
- [37] D. Boschetto, E. G. Gamaly, A. V. Rode, B. Luther-Davies, D. Glijer, T. Garl, O. Albert, A. Rousse, and J. Etchepare, Small Atomic Displacements Recorded in Bismuth by the Optical Reflectivity of Femtosecond Laser-Pulse Excitations, *Phys. Rev. Lett.* **100**, 027404 (2008).
- [38] E. Uykur, B. Ortiz, O. Iakutkina, M. Wenzel, S. Wilson, M. Dressel, and A. Tsirlin, Low-energy optical properties of the nonmagnetic kagome metal  $\text{CsV}_3\text{Sb}_5$ , *Phys. Rev. B* **104**, 045130 (2021).
- [39] X. Chen, X. Zhan, X. Wang, J. Deng, X.-B. Liu, X. Chen, J.-G. Guo, and X. Chen, Highly robust reentrant superconductivity in  $\text{CsV}_3\text{Sb}_5$  under pressure, *Chin. Phys. Lett.* **38**, 057402 (2021).
- [40] H. J. Sielcken and H. J. Bakker, Probing the ultrafast electron and lattice dynamics of gold using femtosecond mid-infrared pulses, *Phys. Rev. B* **102**, 134301 (2020).
- [41] H. Chen, H. Yang, B. Hu, Z. Zhao, J. Yuan, Y. Xing, G. Qian, Z. Huang, G. Li, and Y. Ye, Roton pair density wave in a strong-coupling kagome superconductor, *Nature (London)* **599**, 222 (2021).

- [42] D. H. Torchinsky, F. Mahmood, A. T. Bollinger, I. Božović, and N. Gedik, Fluctuating charge-density waves in a cuprate superconductor, *Nat. Mater.* **12**, 387 (2013).
- [43] R. Yusupov, T. Mertelj, V. V. Kabanov, S. Brazovskii, P. Kusar, J.-H. Chu, I. R. Fisher, and D. Mihailovic, Coherent dynamics of macroscopic electronic order through a symmetry breaking transition, *Nat. Phys.* **6**, 681 (2010).
- [44] J. Demsar, K. Biljaković, and D. Mihailovic, Single Particle and Collective Excitations in the One-Dimensional Charge Density Wave Solid  $K_{0.3}MoO_3$  Probed in Real Time by Femtosecond Spectroscopy, *Phys. Rev. Lett.* **83**, 800 (1999).
- [45] Y. Han, J. Yu, H. Zhang, F. Xu, K. Peng, X. Zhou, L. Qiao, O. V. Misochko, K. G. Nakamura, and G. M. Vanacore, Photoinduced ultrafast symmetry switch in SnSe, *J. Phys. Chem. Lett.* **13**, 442 (2022).
- [46] J. Yu, Y. Han, H. Zhang, O. V. Misochko, K. G. Nakamura, and J. Hu, Attosecond-resolved coherent control of lattice vibrations in thermoelectric SnSe, *J. Phys. Chem. Lett.* **13**, 2584 (2022).
- [47] L. Wang, Y. Han, J. Yu, F. Xu, H. Zhang, C. Gong, H. Lei, and J. Hu, Absence of Kondo effect in CeNiGe<sub>3</sub> revealed by coherent phonon dynamics, *Phys. Rev. B* **104**, 205133 (2021).
- [48] H. Li, T. Zhang, T. Yilmaz, Y. Pai, C. Marvinney, A. Said, Q. Yin, C. Gong, Z. Tu, and E. Vescovo, Observation of Unconventional Charge Density Wave without Acoustic Phonon Anomaly in Kagome Superconductors  $AV_3Sb_5$  ( $A = Rb, Cs$ ), *Phys. Rev. X* **11**, 031050 (2021).
- [49] N. Ratcliff, L. Hallett, B. R. Ortiz, S. D. Wilson, and J. W. Harter, Coherent phonon spectroscopy and interlayer modulation of charge density wave order in the kagome metal  $CsV_3Sb_5$ , *Phys. Rev. Mater.* **5**, L111801 (2021).
- [50] H. Schaefer, V. V. Kabanov, M. Beyer, K. Biljakovic, and J. Demsar, Disentanglement of the Electronic and Lattice Parts of the Order Parameter in a 1D Charge Density Wave System Probed by Femtosecond Spectroscopy, *Phys. Rev. Lett.* **105**, 066402 (2010).
- [51] M. Porer, U. Leierseder, J.-M. Ménard, H. Dachraoui, L. Mouchliadis, I. Perakis, U. Heinzmann, J. Demsar, K. Rossnagel, and R. Huber, Non-thermal separation of electronic and structural orders in a persisting charge density wave, *Nat. Mater.* **13**, 857 (2014).
- [52] R. Yusupov, T. Mertelj, J.-H. Chu, I. Fisher, and D. Mihailovic, Single-Particle and Collective Mode Couplings Associated with 1-and 2-Directional Electronic Ordering in Metallic  $RTe_3$  ( $R = Ho, Dy, Tb$ ), *Phys. Rev. Lett.* **101**, 246402 (2008).
- [53] M. Hase, M. Kitajima, A. M. Constantinescu, and H. Petek, The birth of a quasiparticle in silicon observed in time–frequency space, *Nature (London)* **426**, 51 (2003).
- [54] J. Yu, Y. Han, H. Zhang, X. Ding, L. Qiao, and J. Hu, Excimer Formation in the Non-Van-Der-Waals 2D Semiconductor  $Bi_2O_2Se$ , *Adv. Mater.* **34**, 2204227 (2022).
- [55] J. Yu, Y. Han, L. Wang, F. Xu, H. Zhang, Y. Yu, Q. Wu, and J. Hu, Visualizing nonlinear phononics in layered  $ReSe_2$ , *J. Phys. Chem. Lett.* **12**, 5178 (2021).
- [56] Q. Liu, D. Wu, Z. Li, L. Shi, Z. Wang, S. Zhang, T. Lin, T. Hu, H. Tian, and J. Li, Photoinduced multistage phase transitions in  $Ta_2NiSe_5$ , *Nat. Commun.* **12**, 2050 (2021).
- [57] H. M. Bretscher, P. Andrich, P. Telang, A. Singh, L. Harnagea, A. K. Sood, and A. Rao, Ultrafast melting and recovery of collective order in the excitonic insulator  $Ta_2NiSe_5$ , *Nat. Commun.* **12**, 1699 (2021).
- [58] X. Luo, D. Obeysekera, C. Won, S. H. Sung, N. Schnitzer, R. Hovden, S. W. Cheong, J. Yang, K. Sun, and L. Zhao, Ultrafast Modulations and Detection of a Ferro-Rotational Charge Density Wave Using Time-Resolved Electric Quadrupole Second Harmonic Generation, *Phys. Rev. Lett.* **127**, 126401 (2021).
- [59] A. W. Tsen, R. Hovden, D. Wang, Y. D. Kim, J. Okamoto, K. A. Spoth, Y. Liu, W. Lu, Y. Sun, and J. C. Hone, Structure and control of charge density waves in two-dimensional  $1T'$ - $TaS_2$ , *Proc. Natl. Acad. Sci. USA* **112**, 15054 (2015).
- [60] V. R. Morrison, R. P. Chatelain, K. L. Tiwari, A. Hendaoui, A. Bruhács, M. Chaker, and B. J. Siwick, A photoinduced metal-like phase of monoclinic  $VO_2$  revealed by ultrafast electron diffraction, *Science* **346**, 445 (2014).
- [61] M. Zhang, Z. Wang, Y. Li, L. Shi, D. Wu, T. Lin, S. Zhang, Y. Liu, Q. Liu, and J. Wang, Light-Induced Subpicosecond Lattice Symmetry Switch in  $MoTe_2$ , *Phys. Rev. X* **9**, 021036 (2019).
- [62] E. J. Sie, C. M. Nyby, C. Pemmaraju, S. J. Park, X. Shen, J. Yang, M. C. Hoffmann, B. Ofori-Okai, R. Li, and A. H. Reid, An ultrafast symmetry switch in a Weyl semimetal, *Nature (London)* **565**, 61 (2019).
- [63] S. Meng and E. Kaxiras, Real-time, local basis-set implementation of time-dependent density functional theory for excited state dynamics simulations, *J. Phys. Chem. Lett.* **129**, 054110 (2008).
- [64] W. Ma, J. Zhang, L. Yan, Y. Jiao, Y. Gao, and S. Meng, Recent progresses in real-time local-basis implementation of time dependent density functional theory for electron–nucleus dynamics, *Comput. Mater. Sci.* **112**, 478 (2016).
- [65] C. Lian, M. Guan, S. Hu, J. Zhang, and S. Meng, Photoexcitation in solids: First-principles quantum simulations by real-time TDDFT, *Adv. Theor. Simul.* **1**, 1800055 (2018).
- [66] S. Grimme, Semiempirical GGA-type density functional constructed with a long-range dispersion correction, *J. Comput. Chem.* **27**, 1787 (2006).
- [67] V. Barone, M. Casarin, D. Forrer, M. Pavone, M. Sambri, and A. Vittadini, Role and effective treatment of dispersive forces in materials: Polyethylene and graphite crystals as test cases, *J. Comput. Chem.* **30**, 934 (2009).
- [68] H. J. Monkhorst and J. D. Pack, Special points for Brillouin-zone integrations, *Phys. Rev. B* **13**, 5188 (1976).
- [69] A. Dal Corso, Pseudopotentials periodic table: From H to Pu, *Comput. Mater. Sci.* **95**, 337 (2014).
- [70] J. P. Perdew and A. Zunger, Self-interaction correction to density-functional approximations for many-electron systems, *Phys. Rev. B* **23**, 5048 (1981).